Manuscript refereed by Dr Antonio Romero, Sintermetal SA

Powder Injection Moulding of Functional Ceramic Components for Solid Oxide Fuel Cells

A. Zryd, H. Girard, A. Faes, E. Carreño-Morelli
Design & Materials Unit, University of Applied Sciences Western Switzerland, CH-1950 Sion

Abstract

Solid Oxide Fuel Cells (SOFC) are a promising technology for high efficiency energy conversion. Powder injection moulding (PIM) is a possible approach to reduce the fabrication costs of SOFC. Components in the form of bars and disks with an intricate pattern of small details have been produced by injection moulding of nickel oxide (NiO) and yttria-stabilised zirconia (YSZ). Their residual porosity after sintering and after reduction has been characterised, as a function of sintering parameters. In addition, their thermal behavior and electrical properties have been analysed.

Introduction

Fuel Cells are a promising technology for energy production and high density energy storage. Powder processing is a possible approach to reduce the fabrication costs of Polymer Electrolyte Membrane fuel cells [1, 2, 3] and potentially also for Solid Oxide Fuel Cells (SOFC). Powder injection moulding (PIM) is in particular a production process allowing the fabrication of complex 3-dimensional net ore near-net shapes in an industrial way, with metallic, ceramic and composite materials. Depending on processing parameters, it is also possible to obtain porosity gradients and porous/dense combinations which can be useful for several applications, among others fuel cells [4]. PIM seems therefore a promising route to fabricate Solid Oxide Fuel Cell components, based on a thin electrolyte of yttria-stabilised zirconia (YSZ) supported by an anode composed of nickel oxide (NiO) and YSZ, in an industrial way.

A number of questions however are still open, such as the influence of the large amount of binder required for injection moulding on component properties [5] or the possibility of obtaining precise details in the anode support structure using standard powder. The aim of this preliminary work is to evaluate the feasibility of this approach, from a material standpoint. In particular it is intended to validate the porosity and the electrical resistivity of injected composite materials.

Material and method

The material used for this study was a mixture of 58 wt% Nickel Oxide (Green oxide, Std grade, 14-18 µm particles made up of three dimensional chains of smaller 2-3 µm sub-particles, Novamet Specialty Products Corp., Wyckoff, USA) and 42 wt% Zirconia stabilised by 8 mol% Y_2O_3, 8YSZ
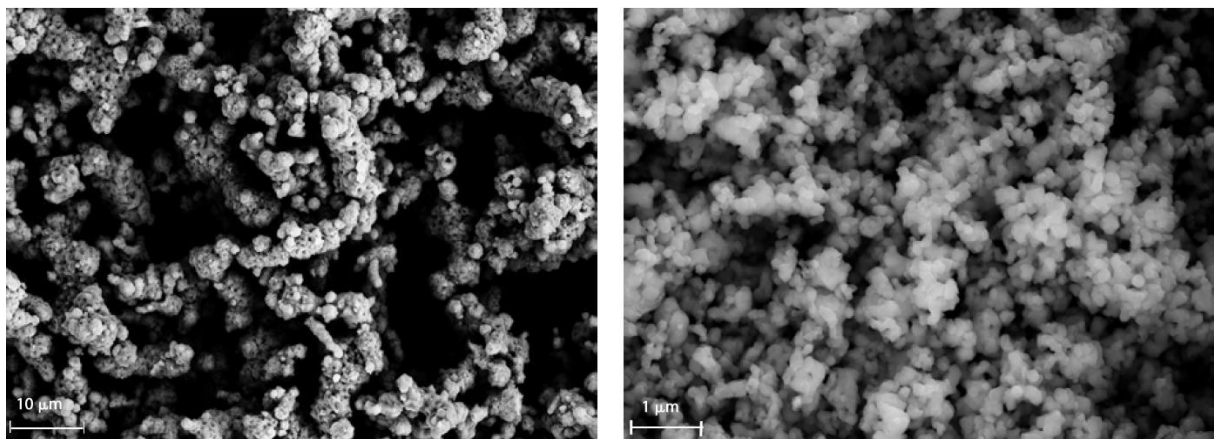

Fig. 1 SEM characterisation of the raw powders. On the left: Green nickel oxide (Novamet) showing particle chains up to 14 - 18 µm length, made up by smaller sub-particles. On the right: Yttria stabilised zirconia (MELChem), with agglomerates of 0.5 to 1 µm.

(MELox 8YF, average particle size 0.5 µm, MEL Chemicals, Manchester, UK). This ratio has been chosen according to [6]. The morphology of the powder can be seen on fig. 1 where the agglomeration of the particles is clearly visible. A feedstock was prepared by mixing these powders in a Coperion LUK 1.0 sigma blade mixer (Werner & Pfleiderer, Stuttgart, Germany) during 2 h at 140 °C, using paraffin wax (PW purum ; pellets, Sigma-Aldrich Chemie GmbH, Buchs, Switzerland), stearic acid (SA, Fluka purum ; >97%, Sigma-Aldrich Chemie GmbH,Buchs, Switzerland) and low density polyethylene (LDPE Riblene MP30; Polimeri Europa, San Donato Milanese, Italy) as a binder, in proportions according to [7] and given in Table 1. Granulation was performed by cooling down and crushing the mixture by slow shearing. The thermal characteristics of this feedstock, as well as of the sintered and reduced components, were assessed by dilatometry, in air, heating rate 10 °C/min (DIL 402E Netzsch Gerätebau GmbH, Selb, Germany).

Component	Powder		Binder		
	NiO	**Y$_8$TZP**	**LDPE**	**SA**	**PW**
Weight (g)	580.0	420.0	41.0	10.9	64.5
Vol%	30.4	24.6	15.7	4.5	24.8
Vol % global	55.0		45.0		

Table 1: Feedstock formulation for 1 kg of ceramic powder.

Simple test bars (5 x 5 x 40 mm) and a more complex disk of diameter 40 mm with small patterns of height 0.3 mm and lateral top dimension 0.6 mm (fig. 2) were injection moulded in an Arburg machine 221K 350-100 (Arburg GmbH + Co KG, Lossburg, Germany) (fig. 2). Mould temperature was about 40 °C. For the disk-shaped specimen, the moulding was performed in a partial vacuum to improve the filling of the details. After shaping, all specimens were subjected to a preliminary solvent debinding step in heptane (24 h at 50°C) to dissolve the paraffin wax and the stearic acid. Thermal debinding and sintering were performed in air in a high-temperature sintering oven (Nabertherm HT 16/17, Nabertherm GmbH, Lilienthal, Germany) as a single thermal cycle: 1 h at 500 °C for a slow degradation of the LDPE backbone and 1 h at 4 different temperatures (1150 °C, 1250 °C, 1350 °C and 1450 °C, heating rate of 180 °C /h) for sintering in order to assess the porosity level of the material. The obtained ceramics were finally subjected to a postprocessing treatment in a different oven (Nabertherm VHT 08/16-Mo, Nabertherm GmbH, Lilienthal, Germany) for 12 h at 800 °C in a H$_2$ atmosphere to reduce the NiO to metallic nickel.
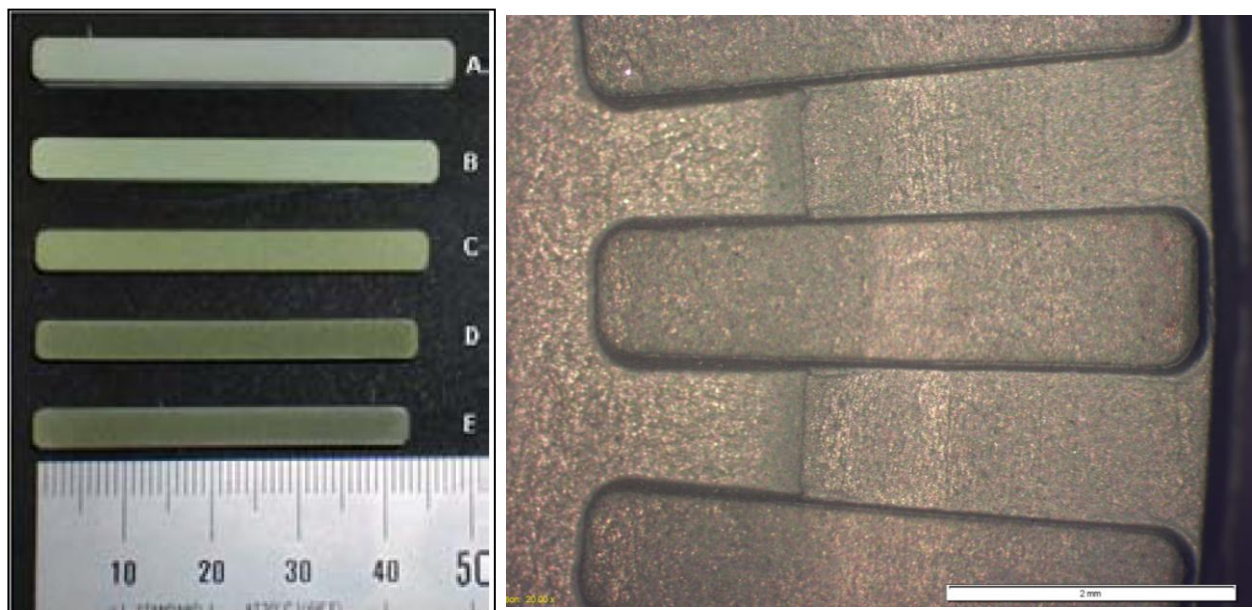

Fig. 2: Injection moulded bars in various states: A: green body, from B to E, as sintered, at respectively 1150 °C, 1250 °C, 1350 °C, 1450 °C (left) and detail of the smaller patterns in a sintered part. The height of the walls is 0.3 mm and their top width 0.6 mm (right).
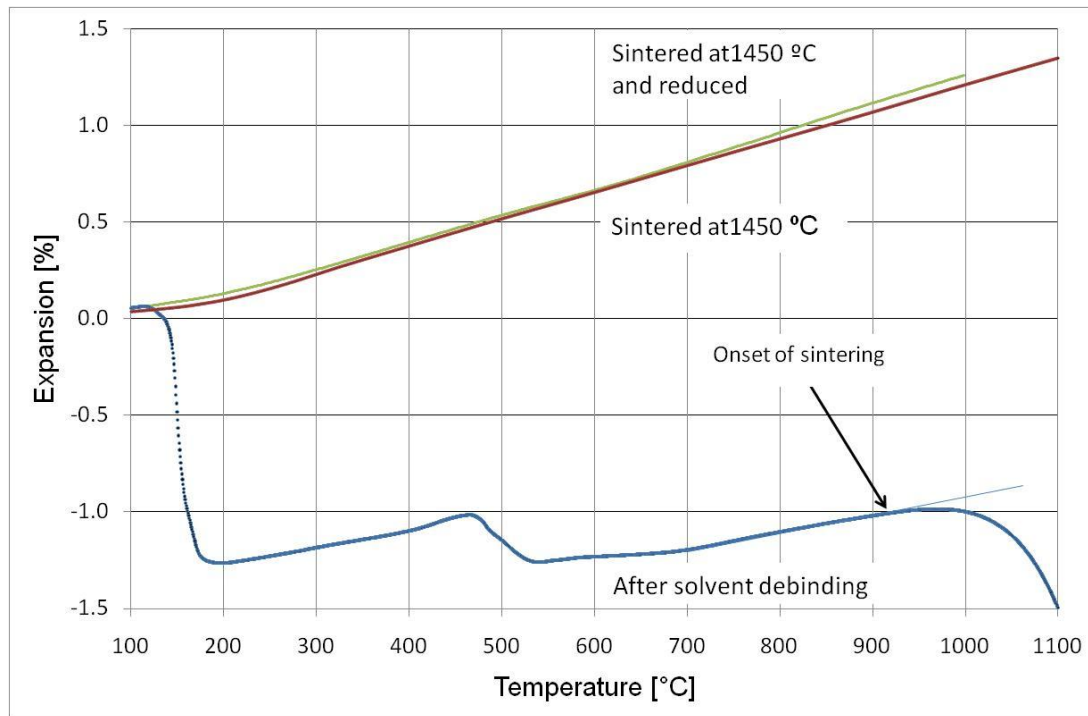
Fig 3. Expansion of the NiO-8%YSZ specimen in a green state (after solvent debinding, bottom), after sintering and after sintering and reduction, in air.

The porosity of the specimens was measured by the Archimedes method and by Helium pycnometry (Multivolume Pycnometer 1305, Micromeritics Instrument Corporation, Norcross, USA). The first approach gives an upper estimate of the closed porosity, the value being overestimated by the incomplete penetration of water in the sample pores. The open porosity was further deduced from the overall volume obtained by geometrical evaluation and by an Archimedes density measurement on an impregnated sample. Scanning electron microscope (SEM) observations (LEO 1525 equipped with a Gemini column, Carl Zeiss Inc., Thornwood, USA) and Energy dispersive X-ray spectroscopy (EDS) (Oxford 7426) analysis of rupture surfaces were done to assess the microstructure and the composition of the samples after sintering and after reduction. Finally, the electrical characteristics of the porous material (after reduction) have been measured by 4 points resistivity.

Results and discussion

The linear shrinkage, measured on the bars after sintering, is varying between 4 % for a sintering temperature of 1150 °C and 12 % at 1450 °C (see fig. 2 and table 2). It is further confirmed by the dilatometric study (fig. 3), which clearly shows the debinding stages (paraffin wax at around 150 °C and LDPE at 500 °C) resulting in a shrinkage of app. 2 % as well as the onset of sintering at app. 950 °C, with a final shrinkage of app. 9% at the maximum achievable temperature of 1300 °C. With a decreasing sintering temperature, the closed porosity is raising from 5 % to 10 %, and the open porosity from 16 % to 34 %. After the reduction, the open porosity increases due to oxygen losses in the material and reaches 35 % to 51 %. A porosity of about 40% would enable to reach good performance by decreasing the gas diffusion losses at the anode [8]. This combination of shrinkage and porosity is similar to the optimal values obtained by tape-casting a similar material [9] and is therefore promising.

The dilatometric study of the green specimen clearly shows the debinding steps (Fig. 3). The first, at around 150 ºC is due to the elimination of incompletely dissolved wax and stearic acid. The second, at 500 ºC, corresponds to the thermal degradation of the LDPE. Finally the onset of sintering is visible at 900 ºC. At 1300 ºC, the sintering shrinkage is 9% and corresponds to the value observed during normal oven sintering. An average coefficient of thermal expansion (CTE) is calculated for the sintered samples between RT and 1000 ºC, according to [10]. It value is $12.4 \cdot 10^{-6}$ ºK^{-1} for the non reduced sample and $13.5 \cdot 10^{-6}$ ºK^{-1} for the reduced sample. The higher TEC in the latter case indicates oxidation of the nickel in air. When this specimen is held 15 min at 1000 ºC, the CTE raises up to
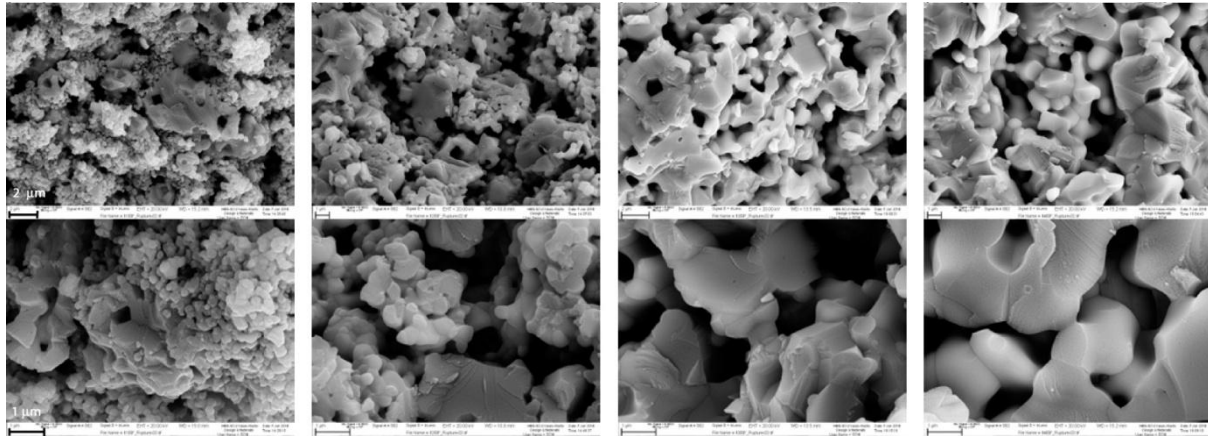
Fig. 4. SEM observations of rupture surfaces of the injected bars, at 4 various sintering temperatures (1150 °C, 1250 °C, 1350 °C and 1450 °C, from left to right) and 2 different magnifications (above, scale bar 2 µm, below, scale bar 1 µm).

$14.7 \cdot 10^{-6}$ °K^{-1} because of further oxidation. These CTE values are well within the expected values from [10], for our ratio of NiO vs YSZ.

Fig. 4 shows the microstructure of rupture surfaces within the bar specimen, at the four different sintering temperatures. Grain growth and an increasing average pore size can be clearly seen. An EDS analysis gives an average sample composition reasonably close to the theoretical values. The observed discrepancy is within the measurement uncertainty, and the results must be taken with care as the measurement surface is a rupture surface. However a mapping of the Ni and Zr has also shown an homogeneous repartition of the elements. This is important, as the efficiency of a SOFC is directly linked to the density of triple boundaries between Ni, Zr and the percolating gas.

Sintering temperature (°C)	Shrinkage after sintering (%)	Porosity after sintering			Electrical conductivity at RT (S/cm)
		Closed (%)	Open (%)	Open, after oxide reduction (%)	
1150	4.2	10 (4)	34 (38)	51	92
1250	7.4	8 (4)	28 (30)	44	1375
1350	10.4	7 (0)	22 (28)	39	3012
1450	12.3	5 (0)	16 (22)	35	4282

Table. 2 : Shrinkage, porosity and room temperature electrical conductivity of the injected bars, for various sintering temperatures. The values for the porosity correspond respectively to the density and the pycnometry measurements (between brackets).

The room temperature electrical conductivity of samples sintered at different temperatures has been measured at room temperature (table 2). It increases from 92 S/cm at 1150 °C to 4282 S/cm at 1450 °C. If a reasonable conductivity loss of 80 % is assumed between RT and 800 °C, the operating temperature of the SOFC (see [9] for a justification of this ratio), the expected conductivity of 18 to 856 S/cm at the operating temperature of a SOFC (typically 800 °C) are well within the values reported by other authors (see e.g. [11]). For the three higher sintering temperatures, the resistivity is above 100 S/cm (equivalent to 500 S/cm at RT), considered a limit for practical use of this material as a SOFC anode. For an anode thickness of 1.2 mm and an active area of 1 cm^2, it indeed corresponds to an ohmic loss of 1.2 mV, i.e. 0.1 % of the SOFC open circuit voltage around 800 °C under humidified H_2 [12].